Accuracy of Boundary Layer Temperature Profiles Retrieved With Multifrequency Multiangle Microwave Radiometry

Susanne Crewell, *Member, IEEE*, and Ulrich Löhnert

***Abstract*—The potential of a ground-based microwave temperature profiler to combine full tropospheric profiling with high-resolution profiling of the boundary layer is investigated. For that purpose, statistical retrieval algorithms that incorporate observations from different elevation angles and frequencies are derived from long-term radiosonde data. A simulation study shows the potential to significantly improve the retrieval performance in the lowest kilometer by combining angular information from relatively opaque channels with zenith-only information from more transparent channels. Observations by a state-of-the-art radiometer employed during the International Lindenberg Campaign for Assessment of Humidity and Cloud Profiling Systems and Its Impact on High-Resolution Modeling (LAUNCH) in Lindenberg, Germany, are used for an experimental evaluation with observations from a 99-m mast and radiosondes. The comparison not only reveals the high accuracy achieved by combining angular and spectral observations (overall, less than 1 K below 1.5 km), but also emphasizes the need for a realistic description of radiometer noise within the algorithm. The capability of the profiler to observe the height and strength of low-level temperature inversions is highlighted.**

***Index Terms*—Atmospheric boundary layer (ABL) profiles, ground-based microwave radiometry, remote sensing, vertical resolution.**

I. Introduction

MICROWAVE profilers that measure several frequencies along the 60-GHz oxygen absorption complex are well established for observing the atmospheric temperature profile from the ground as well as from space. From the ground, observations are typically taken in zenith direction at about five to ten frequency channels from 50–60 GHz [1]. The root mean square (rms) accuracy of this method is about 0.6 K close to the surface and degrades to about 1.5–2 K in the middle troposphere [2]–[4]. The vertical resolution is often defined as the half-width of the vertical interlevel covariance function of the retrieval errors, which decreases rapidly from about 500 m at a height of 300 m to 1 km at a height of 500 m [2], [3].

Manuscript received June 6, 2006; revised October 4, 2006. This work was supported in part by the EU project African Monsoon Multidisciplinary Analyses in preparation for the Humidity and Temperature Profiler (HATPRO) deployment to Africa.

The authors are with the Meteorological Institute, Ludwig-Maximilians-University of Munich, 80539 Munich, Germany, and also with the Institute for Geophysics and Meteorology, University of Cologne, 50923 Cologne, Germany (e-mail: crewell@meteo.uni-koeln.de; loehnert@meteo.uni-koeln.de).

Digital Object Identifier 10.1109/TGRS.2006.888434

Because the development of the atmospheric boundary layer (ABL) is of special interest due to the large transfer of energy between the surface and the atmosphere, a high vertical resolution is desired. Therefore, one-channel systems operating around 60 GHz have been developed [5], [6], which derive profile information from elevation scanning. By assuming horizontal homogeneity of the atmosphere, the observed radiation systematically originates from higher altitudes the higher the elevation angle is. Since these brightness temperatures (TBs) vary only slightly with elevation angle, the method requires a highly sensitive radiometer that is typically realized by using wide bandwidths up to 4 GHz. The resulting vertical resolution has been estimated using the Dirac delta function to decrease from 8 m at a height of 10 m to about 300 m at a height of 400 m and improve the accuracy better than 1 K by comparison with observations from a 300-m tower [7]. The use of a single highly opaque channel limits the information content to altitudes below 600 m.

To extend the vertical range of the ABL temperature profiles, frequency channels with less opacity need to be used. Cadeddu *et al.* [8] performed a theoretical study through a multiresolution wavelet technique for different radiometer configurations, e.g., angles, channels, and bandwidths. Her simulations suggest that the scanning configuration with high sensitivity (large bandwidths) is favorable for altitudes below 1 km; whereas, for altitudes above 1 km, a multifrequency system with fixed elevation gave a better performance.

In this paper, we investigate whether state-of-the-art microwave radiometers can observe an optimal temperature profile throughout the atmosphere by a combination of spectral and angular information. For this purpose, the microwave radiometer Humidity and Temperature Profiler (HATPRO) (Section II) and its characteristics are used first in a simulation study (Section III) to describe the theoretical retrieval performance. Second, an experimental validation (Section IV) with observations from the International Lindenberg Campaign for Assessment of Humidity and Cloud Profiling Systems and Its Impact on High-Resolution Modeling (LAUNCH) 2005 in Lindenberg, Germany, is performed before final conclusions are drawn (Section V).

II. Microwave Radiometer

HATPRO [9] was designed as a network-suitable low-cost microwave radiometer that can observe liquid water path

TABLE I
HATPRO RECEIVER PROPERTIES

Center Frequency (GHz)	Bandwidth τ (MHz)	Channel Sensitivity ΔT_B[a] (K)	Bias[b] T_B-T_{Rs} (K)	St. dev.[b] T_B-T_{Rs} (K)
58.00	2000	0.007	0.24	0.43
57.30	1000	0.009	-0.06	0.39
56.66	600	0.012	-0.04	0.38
54.94	250	0.018	-1.02	0.24
53.86	250	0.018	-.27	0.58
52.28	250	0.018	-0.41	0.96
51.26	250	0.018	3.21	0.98

[a]channel sensitivity is calculated for a Dicke type system with a noise temperature T_{sys}=800 K and an integration time Δt=30 s via the radiometer formulae $\Delta T_B = 2\cdot T_{sys}/(\Delta t\cdot\tau)^{1/2}$

[b]Bias and standard deviation are calculated from a set of 53 radiosoundings launched at Lindenberg using the Rosenkranz gas absorption model [10]

(LWP), humidity, and temperature profiles with high (1 s) temporal resolution. HATPRO comprises total-power radiometers utilizing direct detection receivers within two bands. The first band contains seven channels from 22.335–31.4 GHz, and the second band contains seven channels from 51–58 GHz. The receivers of each frequency band are designed as filter banks to acquire each frequency channel in parallel. In addition, this approach allows setting each channel bandwidth individually. Because profiling the ABL temperature depends strongly on the sensitivity and accuracy of the channels close to the oxygen band center, the channels from 56.66 to 58.00 GHz have a much larger bandwidth than those at lower opacity (standard 250 MHz; see Table I).

The antenna beamwidth for the channels along the oxygen line is 2° full-width at half-maximum with a sidelobe suppression better than 30 dB. Because more than 99.9% of the received power stems from an angular range of ±3°, problems with surface contamination are avoided even at the lowest elevation angle of 5° considered here. The radiometer is enclosed in a radome, which is protected from dew formation by a strong blower system. Precipitating conditions are reported by a precipitation detector. Furthermore, environmental sensors for temperature, humidity, and pressure, as well as a GPS clock, are present.

The absolute radiometer calibration is performed once at the start of a campaign using a liquid nitrogen target and continuously for the channels along the water vapor line using the tipping curve procedure. Relative calibration (gain adjustment) is performed every 5 min by looking at the built-in ambient load.

III. SIMULATION OF RETRIEVAL PERFORMANCE

Statistical retrieval algorithms were developed in a similar fashion as described in detail by Löhnert and Crewell [11], [12]. Basically, a large radiosounding data set is used to generate synthetic TB via radiative transfer calculations together with the corresponding temperature profiles. A multiple linear regression between TB and atmospheric temperature is derived for each height from a training data set and evaluated on the basis of a test data set. Some important considerations in this process are described as follows.

The database consists of more than 10 000 Lindenberg radiosoundings from 1994 to 2002 with high vertical resolution.

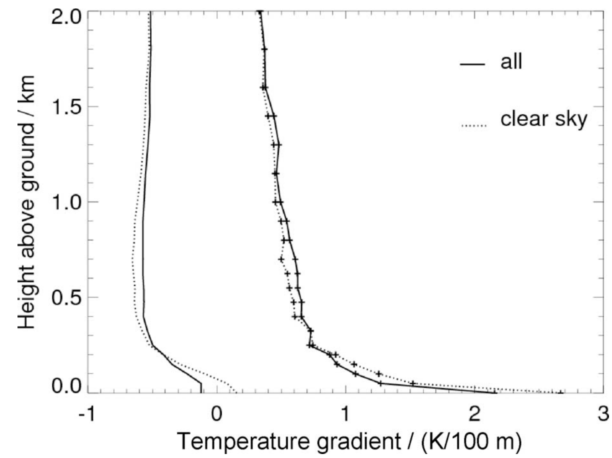

Fig. 1. Mean temperature gradient of radiosonde data set and its standard deviation (+). During clear-sky scenes (dotted line), temperature gradients show highest values close to the surface.

The analysis of the soundings emphasizes the importance of the surface as the largest temperature variations occur close to it (Fig. 1). The surface temperature itself results from the equilibrium of the energy fluxes (net radiation, heat conduction into the ground, and sensible and latent heat). The ABL is, in contrast to the free troposphere, mostly affected by the surface. Its height can vary between a few tens of meters (nighttime stable ABL) to up to 4 km (free convective ABL), depending on turbulence and static stability. On the average, the Lindenberg soundings show a typical temperature gradient of about −0.6 K/100 m above a height of 300 m. For lower heights, the gradient approaches zero at the ground. Clear-sky cases were separated from cloudy ones by only considering profiles where the relative humidity never exceeded 95%. For these cases, the mean temperature gradient even becomes positive when close to the ground, indicating the frequent occurrence of temperature inversions caused by radiative cooling during the night.

The data are divided into a training $(N = 5334)$ and a test $(N = 4954)$ data set. For each sounding, the radiative transfer for all HATPRO frequencies was calculated based on the Rosenkranz gas absorption model [10]. We chose, in total, six elevation angles, i.e., 90.0°, 42.0°, 30.0°, 19.2°, 10.2°, and 5.4°, corresponding to air mass factors of about 1, 1.5, 2, 3, 5, and 10, respectively. Algorithms were developed on a 50-m vertical grid close to the ground, which gradually degrades to 1 km in the upper troposphere. Note that this grid is finer than the true vertical resolution of the retrievals but similar to the one used by current weather forecast models.

The variation of the simulated TB with the angle is rather small; in 50% of all cases, the TB variation between 5.4° and 90° is less than 1.8 K at 58 GHz (2.1 K at 57.3 GHz, 2.4 K at 56.66 GHz, and 6.9 K at 54.94 GHz). When the angular range is reduced, i.e., the lowest angle is limited to 10.2°, this value is reduced to 1.6 K at 58 GHz. This emphasizes that a highly accurate and stable radiometer is needed to resolve the TB variations.

If only the angular information is considered at a single frequency, the three highest frequencies give a similar performance up to about a height of 700 m with an rms error of about 0.7 K. In the lowest 300 m, the error even reduces to

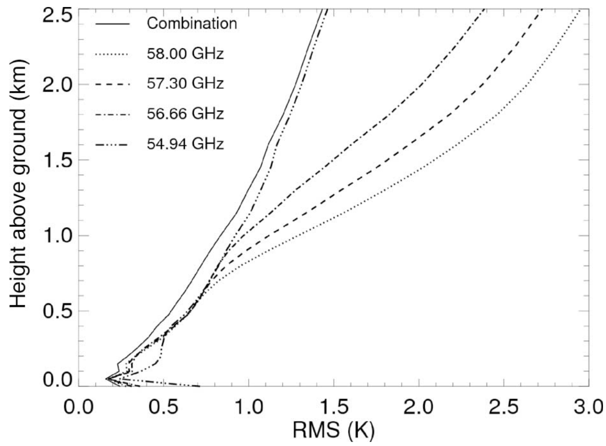

Fig. 2. RMS error of ABL temperature retrievals based on elevation scans (six angles) at four selected frequencies (dashed and dotted lines indicated in the figure). The solid line shows that the combination of TB measured at four frequencies and six angles gives the best performance. The noise level was assumed to be 0.1 K, considering the specifications of the HATPRO frequencies (Table I).

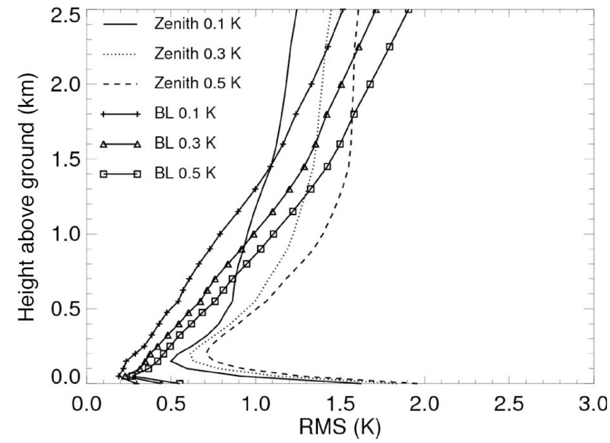

Fig. 3. Performance of temperature retrievals for zenith (seven channels) and ABL scanning (four channels, six angles) mode in terms of rms error. Three different noise levels (0.1, 0.3, and 0.5 K) in TB are assumed.

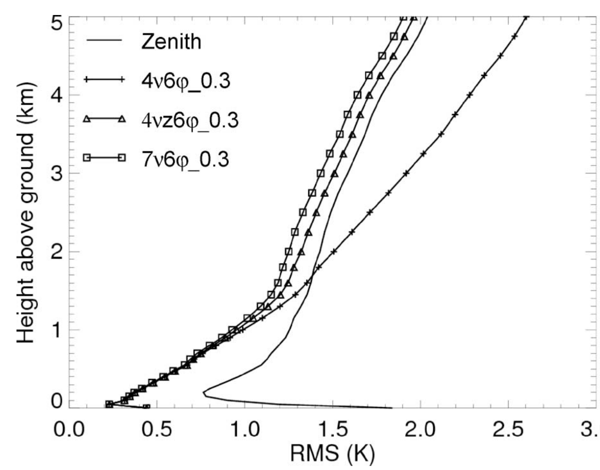

Fig. 4. Performance of ABL temperature retrievals for different combinations of observations. Retrieval nomenclature: $X\nu[z]Y\varphi\_RR$. X: number of frequencies with elevation scanning; Y: number of elevation angles; and RR: noise level in Kelvin. The index z indicates that, additionally, three zenith observations for 51.26–53.86 have been included in retrieval development.

~0.2 K, showing how direct the measurement is related to temperature (Fig. 2). The maximum height with an acceptable rms error of 1 K is at 1 km for the 54.94-GHz channel. This channel, however, already gives a poorer performance at the lower levels. Therefore, no channels with lower opacities have been considered. Clearly, the best performance is achieved when all the frequencies at all the angles are combined in one algorithm, giving an accuracy better than 0.5 K throughout the lowest 500 m. Note the particular retrieval performance at the ground level: here, the surface temperature depends strongly on soil moisture and vegetation properties, which are both highly variable on small scales. Therefore, the turbulent fluxes of sensible and latent heat show strong horizontal variations close to the surface, and the adjacent atmosphere becomes inhomogeneous. However, already at a height of 50 m, which is our next vertical level, the diffusive role of turbulence has led to an effective blending. This decoupling between the surface and the atmosphere is also the reason why no improvement in the temperature retrievals is achieved by incorporating *in situ* measurements of environmental temperature [4].

It should also be noted that, in reality, other problems that are not considered in this simple simulation framework might occur. While close to the absorption center, the opacity is so high that most of the radiation originates from along a path of about 300 m; at 54.94 GHz, this path length increases to about 1–2 km. Especially at the low elevations, very different surfaces, for example, forests, lakes, or concrete, might change the atmospheric temperature profile and make the assumption of horizontal homogeneity invalid.

Now, the following question arises: How does the combined ABL scanning algorithm compare with the standard zenith operation mode? Therefore, for the same data set, a retrieval algorithm making use of all seven HATPRO channels was developed. In this retrieval, we include quadratic terms of TB to take into account the higher nonlinearity of the problem. Close to the surface, this algorithm performs much worse than the angular one (Fig. 3). Within the lowest ~800 m of the atmosphere, the ABL algorithm performs better than the zenith one even if the noise level of the TB is assumed higher than that of the zenith algorithm (0.5–0.1 K). When the same noise level is assumed, the zenith algorithm turns superior at an altitude of about 1500 m. This is about 500 m higher than that indicated by Cadeddu *et al.* [8] and can be attributed to the use of, in total, four frequency channels in the ABL algorithm. Because the ABL often exceeds 1000 m, the improved accuracy should be beneficial to ABL studies.

To get one consistent temperature profile covering the full troposphere, it is clear that more transparent channels need to be included into the retrieval. The simplest way, e.g., to use all HATPRO frequencies and all angles, might be problematic in practice because different air masses might be probed at low elevation angles. Fig. 4 shows that it is sufficient to add the three most transparent channels only with their zenith observations to achieve a similar accuracy as the zenith retrieval at higher altitudes. If only cloud-free conditions are considered, the angle information of the transparent channels is also useful at higher altitudes (more radiation comes from here); even up to an

TABLE II
HATPRO SETTINGS DURING BOTH OBSERVATION PERIODS

	Period A	Period B
Begin (UTC)	8 September 05, 9	17 October 05, 12
End (UTC)	17 September 05, 18	1 November 05, 8
Elevation angles used for BL scans (°)	90.0, 42.0, 30., 19.2, 10.2	90.0, 42.0, 30., 19.2, 10.2, 5.4
BL duration (s)	320	320
BL repetition time (min)	30	20

altitude of 4 km, the accuracy is even up to ∼0.3 K better than the zenith retrieval (not shown).

IV. Experimental Evaluation

A. Intercomparison Data and Setup

To test the retrieval algorithms developed earlier in this paper, we use data from the LAUNCH 2005 campaign at and around the Richard-Aßmann Observatory of the German Weather Service (DWD), Lindenberg, Germany (52.17 N, 14.12 E). The observatory is located ∼65 km southeast of Berlin. Vaisala RS-92 radiosondes are launched operationally four times a day (00, 06, 12, and 18 UTC). DWD further operates a ABL measurement site at Falkenberg, 4 km south of Lindenberg. Here, HATPRO was deployed to compare the retrieved temperature profiles with observations of temperature and humidity taken at six levels (10, 20, 40, 60, 80, and 98 m) along a 99-m mast. The Falkenberg observations are complemented by sonic detection and ranging/radio acoustic sounding system and a ceilometer [13]. The area around Lindenberg and Falkenberg is dominated by farmland, and its altitude varies between 50 and 120 m above sea level.

Microwave radiometer observations were taken at Falkenberg starting on September 8, 2005, 9 UTC and ending on November 1, 2005, 7 UTC. Unfortunately, on September 17, 18 UTC, the GPS clock failed, which led to an omission of relative calibrations until this was corrected for on October 17, 12 UTC. Because the data in this time interval are of poor quality, they are ignored in the following. The instrument settings during the two considered periods (A and B) are given in Table II. The elevation scans lasted about 5 min each with an integration time of about 30 s at each angle. In between the scans, zenith observations for LWP measurements were taken.

B. Comparison With Tower Observations

When the HATPRO observations are compared with the observations of the 99-m mast, one has to be aware of the fact that while the tower sensors integrate at one point for 10 min, HATPRO needs about 5 min for observing the different angles. Therefore, the time series of the mast observations (Fig. 5) show a smoother structure than those of the HATPRO data. Some single spikes occur in the HATPRO observations, which might be caused by obstacles (for example, people working on the field site) or strong precipitation, which has not been filtered out of the data. For the lowest (10 m) and highest (98 m) level

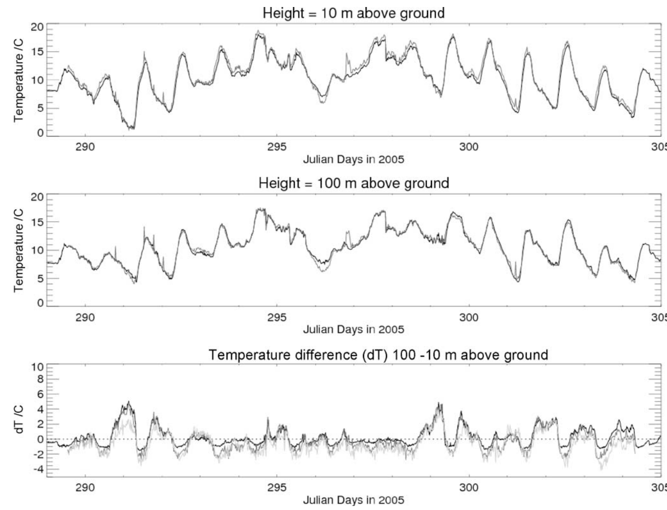

Fig. 5. Time series of (black) mast and (gray) HATPRO observations at the lowest (10 m) and highest (100 m) mast levels, as well as temperature difference between these for observation period B. Retrievals with (gray) six angles and (light gray) five angles.

of the tower, the HATPRO observations match the tower data very well.

Most interesting is the capability of the system to observe the strength of ground-level temperature inversions, which are expressed here as the temperature difference dT between 100 m and the surface (Fig. 5, bottom plot). The overall agreement is very promising, showing that during clear nights, the radiative cooling at the surface can lead to inversions with a temperature increase with a height of more than 4 K. The radiometer observations show a noisier structure, which seems to be stronger during daytime (also in period A, not shown here) and, therefore, might partly be attributed to thermals within the view of the radiometer. For a more quantitative comparison, all tower and HATPRO observations that match within 30 min have been compared (Table III) by means of the standard deviation of the difference between the two (STD). Regarding the $4\nu z6\varphi\_0.1$ retrieval, an STD of 0.53 K (correlation 0.986) at the 100-m level achieved over a large range of atmospheric temperatures (0 °C to 30 °C at ground level) demonstrates an excellent performance. It should be noted that no filtering has been applied, and even rainy scenes are included. The bias between HATPRO and the mast rather strongly depends on the type of retrieval algorithm that is used. A bias close to zero (0.02 K) at 100 m is achieved with the angular information of the highest four frequencies and the zenith measurement of the other three channels, assuming 0.1-K noise level $(4\nu z6\varphi\_0.1)$.

During observation period B, the effect of using six versus five angles can be verified experimentally. When only five angles (down to 10.2°) are used, the STD at a height of 100 m only slightly increases (by about 0.1 K) compared to the six-angle retrieval. However, for the temperature difference, the retrieval quality is reduced much stronger: The STD increases by about 0.3 K, and the correlation decreases from 0.89 to 0.72 (Table III). This not only emphasizes the need for including low-elevation angles, but also puts demands on the angular resolution of the radiometer.

TABLE III

COMPARISON BETWEEN MAST AND HATPRO TEMPERATURE AT 100 m AND dT BETWEEN THE SURFACE AND 100 m IN TERMS OF BIAS, STD, AND CORRELATION (COR) ($X\nu$[z]$Y\varphi\_RR$, WHERE X IS THE NUMBER OF FREQUENCIES WITH ELEVATION SCANNING, Y IS THE NUMBER OF ELEVATION ANGLES, AND RR IS THE NOISE LEVEL IN KELVIN. THE INDEX z INDICATES THAT, ADDITIONALLY, THREE ZENITH OBSERVATIONS FOR 51.26–53.86 HAVE BEEN INCLUDED IN RETRIEVAL DEVELOPMENT)

Algorithm	100m Bias/ K	dT Bias/K	100m STD /K	dT STD /K	100 m Cor	dT Cor
October	*Period B*					
zenith	-1.75	0.36	1.16	1.33	0.929	0.284
4v6φ_0.3	-0.33	0.18	0.57	0.60	0.982	0.894
7v6φ_0.3	-0.21	0.48	0.58	0.64	0.982	0.881
4vz6φ_0.3	-0.53	0.06	0.57	0.60	0.983	0.896
4vz6φ_0.1	0.02	0.46	0.53	0.58	0.986	0.928
4vz5φ_0.3	-0.45	-0.20	0.63	0.94	0.979	0.723
4vz5φ_0.1	-0.04	0.97	0.60	0.84	0.991	0.807
Sept./Oct. 4vz5φ_0.1/ 4vz6φ_0.1	*Period (A+B)*					
all	-0.03	0.45	0.50	0.62	0.993	0.918
no rain	-0.02	0.47	0.50	0.62	0.994	0.921

Observation period B includes very complicated structures in the temperature profiles. Therefore, it would have been misleading to compare the results achieved with the five-angle retrieval in period A with the ones of the six-angle retrieval in period B. As a result, the combined data set (A + B) generally shows a smaller STD (Table III) than that of period B.

The use of all angles at all frequencies ($7\nu6\varphi\_0.3$; see Table III) leads to a minor degradation of accuracy, indicating a slight problem with the assumption of horizontal homogeneity. However, for these lower altitudes, the transparent channels do not contribute strongly to the retrieval, and no firm result can be given here.

C. Comparison With Radiosoundings

To further explore the retrieval quality for higher atmospheric layers, a comparison with the high-quality radiosoundings from Lindenberg was performed. Here, it is most important to investigate to which degree complex temperature structures can be resolved from microwave radiometry. In the lowest ~400 m, where the theoretical accuracy is below 0.5 K and the vertical resolution for a single channel is around 300 m [7], an excellent agreement can be observed (Fig. 6). At higher altitudes, the agreement is still good; however, the degradation in vertical resolution causes an averaging of the temperature profiles to take place. Especially in situations with more than one inversion, only the lowest one can be resolved. These limitations are inherent to the observation technique; however, for some applications like atmospheric model evaluation, this might not pose a strong handicap as long as the vertical resolution can be specified and taken into account.

Lindenberg is located 40 m higher than Falkenberg. Therefore, we compare the radiosonde measurement at 60 m above ground level at Lindenberg with the HATPRO temperature retrieval and the mast observation at 100 m above sea level at Falkenberg. It is important to note that this level is above the typical blending height, and we do not expect deviations due to the fact that the radiosonde only catches a snapshot at that level, whereas HATPRO integrates longer. For the 80 samples matched within ±20 min, the radiosoundings are, on the average, about 0.3 K colder than the mast at Falkenberg with an STD of 0.37 K. In comparison, the difference between HATPRO and the mast has a bias of ~0 K with an STD of ~0.5 K, indicating the similar quality of all observation types for the 100-m temperature.

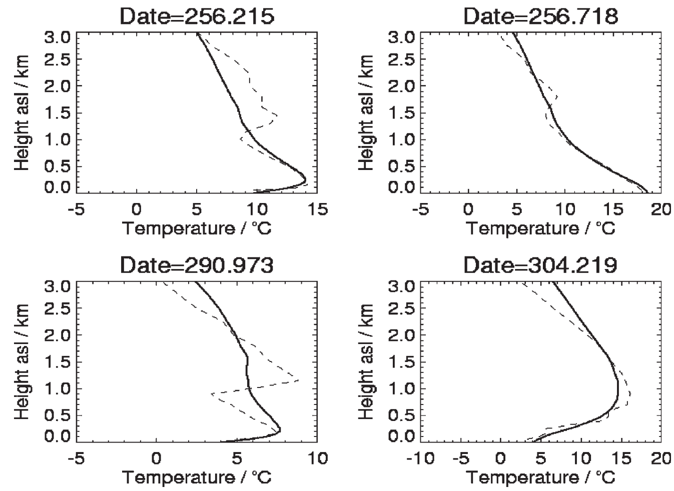

Fig. 6. Comparison of selected HATPRO retrievals with corresponding radiosoundings from Lindenberg (dashed). The height is given above the ground level of Falkenberg.

When higher altitudes are compared, additional discrepancies between radiometer and radiosonde observations can occur due to the spatial difference between the observations. Assuming an average wind speed of 10 m/s, the balloon has drifted about 6 km away from the site when it reaches 3000 m. With Falkenberg already 4 km away from Lindenberg, the maximum difference can be up to 10 km, depending on wind direction. Because the terrain is quite homogeneous grass and farmland, significant differences are only expected in broken cloud situations. Although no degradation in retrieval accuracy occurred in the lowest 100 m during rain events, it is important to eliminate these scenes in the comparisons with radiosondes. The reason is that the emission by rain drops at the transparent frequencies is significant and is not included in the training data set.

The statistical comparison over the whole period shows that the STD is best at 100 m (Fig. 7). The lowest level (50 m) value is slightly worse, because at the corresponding altitude of 10 m in Lindenberg, surface effects play a role. Above 100 m, the STD increases with height to about 1 K at 1 km, staying more or less constant at higher altitudes. Compared to the standard zenith mode, the temperature retrieval using angular information in the lower 2 km is significantly improved. Above 2 km, both algorithms approach each other and perform similar at a higher altitude (not shown). The lower the assumed noise level within the retrieval development, the lower the STD: For the lower 1.5 km, the STD is reduced by about 0.3 K when the assumed noise level is assumed to be 0.1 instead of 0.5 K.

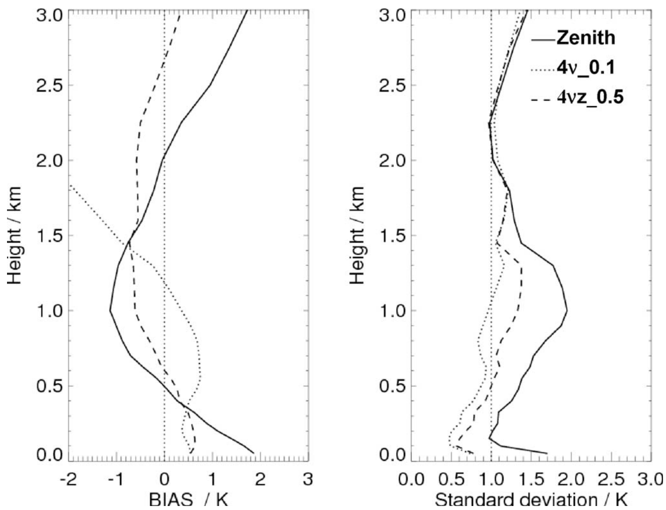

Fig. 7. Comparison of HATPRO retrievals with 80 corresponding radiosoundings from Lindenberg (observation periods A and B) in terms of bias and STD (HATPRO temperature minus sonde temperature). Retrievals were performed (solid) using zenith observations only, $(4\nu\_0.1)$ using the angular information at the four most opaque frequencies, and $(4\nu z\_0.5)$ by further adding the zenith observation by the more transparent channels.

In terms of bias errors, the radiometer observations containing angular information are slightly warmer than the radiosoundings close to the ground, which is consistent with the mast observations. The zenith retrieval gives a much stronger bias, which might be due to bias errors in brightness temperature (Table I). If the angular information of the four most opaque channels is used, the bias increases to unacceptable values above 1.5 km. At these altitudes, hardly any information is contained in the measured TB, and the retrieval relies on the statistics of the training data set. To use only one retrieval algorithm for the full troposphere, the best results were achieved when the three more transparent channels were added with only their zenith observations. It turned out that the best results (lowest bias) were achieved when the noise level of the training data set was at a higher level (0.5 K). If lower values were used (not shown), the bias error increased strongly with height. However, the use of the higher noise level reduces the agreement in terms of STD in the lower 1.5 km. One possibility to improve this might be the use of different noise levels for the different channels. This exercise with real data shows that for statistical retrievals, it is very important to take the bias errors properly into account, as has already been shown in a simulation study [12].

V. Conclusion

For the first time, an excellent all-weather capability of low boundary layer temperature retrievals could be demonstrated for a microwave radiometer, which, at the same time, is able to perform LWP and tropospheric humidity and temperature observations. This can be achieved by adding angular information (down to 5° elevation) at multiple frequencies to the standard zenith observations. A precondition is that the radiometer points over a homogeneous surface. Comparisons with a 99-m mast show that these observations allow an accurate detection of inversions and show a comparable quality of the retrieved temperatures to those of radiosoundings.

To retrieve a consistent temperature profile with the highest accuracy throughout the troposphere, different statistical algorithms were developed. All algorithms, including angular information, achieved an improved performance in the lowest 1.5 km with an STD of less than 1 K to radiosoundings. The best performance throughout the troposphere was achieved when the four most opaque frequencies were used with their angular information and the three more transparent channels were added with only their zenith measurement. For higher altitudes, a strong sensitivity to the noise level in the training data set was found, which resulted in unacceptable bias errors. To further improve the accuracy, a more complex bias analysis of TB needs to be performed. Furthermore, a better information combination might be achieved by a physical retrieval algorithm. Because for that purpose a combination with lidar and cloud radar is desirable [14], the statistical retrievals presented in this paper will be the preferred choice when standalone microwave observations are considered.

Acknowledgment

The authors would like to thank H. Czekala and T. Rose (Radiometer Physics GmbH) for their support in the retrieval development. D. Engelbart, U. Görsdorf, and J. Güldner (DWD) and B. Pospichal are acknowledged for their help in the LAUNCH field campaign.

References

[1] E. R. Westwater, S. Crewell, and C. Mätzler, "A review of surface-based microwave and millimeter wave radiometric remote sensing of the troposphere," *Radio Sci. Bull. URSI*, vol. RSB-310, pp. 59–80, Sep. 2004.

[2] J. Güldner and D. Spänkuch, "Remote sensing of the thermodynamic state of the atmospheric boundary layer by ground-based microwave radiometry," *J. Atmos. Ocean. Technol.*, vol. 18, no. 6, pp. 925–933, Jun. 2001.

[3] J. C. Liljegren, S. A. Boukabara, K. Cady-Pereira, and S. Clough, "The effect of the half-width of the 22-GHz water vapor line on retrievals of temperature and water vapor profiles with a 12-channel microwave radiometer," *IEEE Trans. Geosci. Remote Sens.*, vol. 43, no. 5, pp. 1102–1108, May 2005.

[4] S. Crewell, H. Czekala, U. Löhnert, C. Simmer, T. Rose, R. Zimmermann, and R. Zimmermann, "Microwave radiometer for cloud carthography: A 22-channel ground-based microwave radiometer for atmospheric research," *Radio Sci.*, vol. 36, no. 4, pp. 621–638, 2001.

[5] E. N. Kadygrov and D. R. Pick, "The potential performance of an angular scanning single channel microwave radiometer and some comparisons with *in situ* observations," *Meteorol. Appl.*, vol. 5, pp. 393–404, 1998. DOI: 10.1017/S1350482798001054.

[6] M. W. Rotach, P. Calanca, G. Graziani, J. Gurtz, D. G. Steyn, R. Vogt, M. Andretta, A. Christen, S. Cieslik, R. Conolly, S. F. J. De Wekker, S. Galmarini, E. N. Kadygrov, V. E. Kadygrov, E. Miller, B. Neininger, M. Rucker, E. Van Goersel, H. Weber, A. Weiss, and M. Zappa, "Turbulence structure and exchange processes in an Alpine valley: The Riviera project," *Bull. Amer. Meteorol. Soc.*, vol. 85, no. 9, pp. 1367–1385, 2004.

[7] E. R. Westwater, Y. Han, V. G. Irisov, V. Leuskiy, E. N. Kadygrov, and S. A. Viazankin, "Remote sensing of boundary-layer temperature profiles by a scanning 5-mm microwave radiometer and RASS: Comparison experiment," *J. Atmos. Ocean. Technol.*, vol. 16, no. 7, pp. 805–818, Jul. 1999.

[8] M. P. Cadeddu, G. E. Peckham, and C. Gaffard, "The vertical resolution of ground-based microwave radiometers analyzed through a multiresolution wavelet technique," *IEEE Trans. Geosci. Remote Sens.*, vol. 40, no. 3, pp. 531–540, Mar. 2002.

[9] T. Rose, S. Crewell, U. Löhnert, and C. Simmer, "A network suitable microwave radiometer for operational monitoring of the cloudy atmosphere," *Atmos. Res.*, vol. 75, no. 3, pp. 183–200, 2005.

[10] P. W. Rosenkranz, "Water vapor microwave continuum absorption: A comparison of measurements and models," *Radio Sci.*, vol. 33, no. 4, pp. 919–928, 1998.

[11] U. Löhnert and S. Crewell, "Accuracy of cloud liquid water path from ground-based microwave radiometry—Part I: Dependency on cloud model statistics and precipitation," *Radio Sci.*, vol. 38, no. 3, 8041, 2003. DOI: 10.1029/2002RS002654.

[12] S. Crewell and U. Löhnert, "Accuracy of cloud liquid water path from ground-based microwave radiometry—Part II: Sensor accuracy and synergy," *Radio Sci.*, vol. 38, no. 3, 8042, 2003. DOI: 10.1029/2002RS002634.

[13] U. Görsdorf, F. Beyrich, H. Dier, and U. Leiterer, "Composite wind and temperature profiles obtained from a complex of *in-situ* and remote sensing measurement systems for the forcing of a boundary layer model," *Theor. Appl. Climatol.*, vol. 73, no. 1/2, pp. 97–105, 2002.

[14] U. Löhnert, S. Crewell, and C. Simmer, "An integrated approach towards retrieving physically consistent profiles of temperature, humidity, and cloud liquid water," *J. Appl. Meteorol.*, vol. 43, no. 9, pp. 1295–1307, 2004.

Susanne Crewell (M'06) received the Ph.D. degree in physics from the University of Bremen, Bremen, Germany, in 1993.

From 1994 to 1996, she was with the State University of New York, Stony Brook. Since 2004, she has been with the Ludwig-Maximilians-University of Munich, Munich, Germany, as a Professor of experimental meteorology. Her research interests focus on passive microwave remote sensing of the Earth. She has worked on latent heat flux determination from satellite, observation of stratospheric trace gases from aircraft and ground, as well as tropospheric water vapor, temperature, and hydrometeors. Her current main interests include the combination of observations in different spectral regions and the use of observations for improving atmospheric weather forecast models.

Dr. Crewell is an Associate Editor of the IEEE GEOSCIENCE AND REMOTE SENSING LETTERS.

Ulrich Löhnert received the Ph.D. degree in meteorology from the University of Bonn, Bonn, Germany, in 2002.

From 1998 to 2003, he was a Research Scientist with the University of Bonn, University of Kiel, and the National Oceanic and Atmospheric Administration, Environmental Technology Laboratory. Since 2004, he has been with the Ludwig-Maximilians-University of Munich, Munich, Germany, as an Assistant Professor. In recent years, his research has focused on the development of statistical and physical methods for deriving profiles of the atmospheric thermodynamic state through sensor synergy, as well as on the retrieval of ice microphysical properties.